Intersubband Exciton Relaxation Dynamics in Single-Walled Carbon Nanotubes

C. Manzoni,[1] A. Gambetta,[1] E. Menna,[2] M. Meneghetti,[2] G. Lanzani,[1] and G. Cerullo[1]

[1]*Dipartimento di Fisica, Politecnico di Milano, ULTRAS-INFM, Piazza L. da Vinci 32, 20133 Milan, Italy*

[2]*Department of Chemical Sciences, University of Padova, 1, Via Marzolo, 35131 Padova, Italy*

(Received 19 November 2004; published 23 May 2005)

We study exciton (EX) dynamics in single-walled carbon nanotubes (SWNTs) included in polymethylmethacrylate by two-color pump-probe experiments with unprecedented temporal resolution. In the semiconducting SWNTs, we resolve the intersubband energy relaxation from the EX2 to the EX1 transition and find time constants of about 40 fs. The observation of a photoinduced absorption band strictly correlated to the photobleaching of the EX1 transition supports the excitonic model for primary excitations in SWNTs. We also detect in the time domain coherent oscillations due to the radial breathing modes at ≈ 250 cm^{-1}.

DOI: 10.1103/PhysRevLett.94.207401 PACS numbers: 78.67.Ch, 42.65.-k, 78.47.+p, 78.55.Kz

Single-walled carbon nanotubes (SWNTs) are quasi-one-dimensional (1D) solids made up of enrolled graphene sheets which, depending on their chirality, behave as semiconductors or metals [1]. They have recently aroused a great interest due to their physical properties enabling applications in mechanics [2], nanoelectronics [3,4], and photonics [5]. Bulk amounts of SWNTs contain a mixture of metallic ($\approx 1/3$) and semiconducting ($\approx 2/3$) tubes with different diameters and chiralities. In SWNTs one-dimensional quantum confinement leads to valence and conduction subbands with diverging density of states at the subband edges (van Hove singularities). This prediction ignores Coulomb-correlation effects [6]; however, recent experimental [7] and theoretical [8,9] results point out the relevance of electron-electron interactions in 1D systems, and therefore the importance of considering excitonic effects. Ultrafast optical spectroscopy was used to study carrier relaxation dynamics in SWNTs: This is important for understanding the nature of their primary photoexcitations and also for photonic applications as ultrafast switches. Based on techniques such as time-resolved photoemission [10], pump-probe [11–16] and fluorescence upconversion [17,18], it was found that semiconducting SWNTs excited to their first excitonic state (EX1) exhibit a very fast recovery to the ground state with time constant of ≈ 1 ps, attributed to nonradiative decay. Structured photoinduced absorption (PA) correlated with photobleaching (PB) was observed [14]. When excited to the second excitonic state in the visible (EX2), they relax to the lowest state on a time scale too fast to be temporally resolved [13,14,17].

In this work we study excited state dynamics of SWNTs with a temporal resolution high enough to resolve the intersubband EX2 $\rightarrow$ EX1 relaxation, for which we find a time constant $\tau \cong 40$ fs independent from excitation intensity. We also observe that the PB of the EX1 transition in the IR is always associated with a PA band in the visible, supporting the excitonic model for photoexcitations in SWNTs. Transient oscillations due to coherent excitation of the radial breathing mode of the SWNTs are seen in some time traces.

The experimental setup starts with an amplified Ti:sapphire laser (500 μJ, 150 fs, 1 kHz) driving two noncollinear optical parametric amplifiers (NOPAs) [19]. The first NOPA generates pulses tunable in the near IR (0.8–1.4 eV) with widths ranging from 15 fs at 1.4 eV to 30 fs at 0.92 eV; by frequency doubling, 15 fs pulses at 2.75 eV are obtained. The second NOPA generates visible pulses (1.8–2.4 eV bandwidth) compressed to sub-10 fs duration by chirped mirrors [20]. It is possible either to use a single NOPA for degenerate pump-probe experiments or to synchronize the two NOPAs for two-color experiments. Cross correlation between pump and probe pulses is used to set time zero and determine the instrumental response function. We studied samples of SWNTs grown by the high pressure carbon monoxide procedure (HiPco). Purified HiPco buckytubes (Carbon Nanotechnologies, Inc.) were functionalized with poly(ethylene glycol) (PEG) chains to improve dispersion in a polymer matrix. Derivatization was achieved through amidation of nanotube-bound carboxylic acids with PEG-amine [21]. The functionalized SWNTs were embedded in polymethylmethacrylate films cast on glass cover slips. Resonance Raman spectra showed that the oxidation reaction used for the functionalization destroyed the nanotubes with a diameter below ≈ 0.90 nm [22]. These spectra do not show an increased number of defects in the functionalized samples since the D band (at 1315 cm^{-1}), which depends on the density of defects in the nanotubes [23], has almost the same intensity, with respect to the G band at 1588 cm^{-1}, as in the original nanotubes. Experiments were performed in air at room temperature; excitation intensity was kept in the linear regime, with differential transmission ($\Delta T/T$) below 2%–3%. Figure 1 shows the absorption spectrum of the SWNT sample used for the experiments; the bands are broadened due to the dispersion of absorption energy with tube radius and chirality [7]. Figure 1 also shows spectra of the pulses used in the experiments.

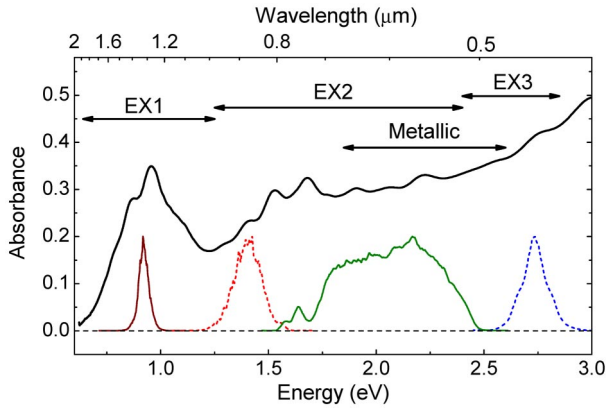

FIG. 1 (color online). Linear optical absorption spectrum of the sample. The energy ranges for first (EX1), second (EX2), and third (EX3) excitonic transition of the semiconducting SWNTs, as well as for the metallic SWNTs, are indicated. Spectra of the different ultrashort pulses used for excitation are also shown.

Figure 2 shows $\Delta T/T$ dynamics at two different probe energies following photoexcitation with a 30 fs pulse at 0.92 eV, resonant with the EX1 transition. At 0.95 eV probe energy [Fig. 2(a)] one observes the prompt rise of EX1 PB, followed by a decay due to interband recombination; exponential fitting gives a time constant $\tau \cong 400$ fs for ground state recovery, in good agreement with previous measurements [13–16]. The recombination dynamics does not show any excitation intensity dependence, as observed in previous studies [15,16], excluding bimolecular exciton annihilation. Tuning the probe wavelength to the visible (2 eV), a PA signal is detected, also instantaneously rising and decaying with the same dynamics as the PB at 0.95 eV. This signal was already observed in SWNTs [13,14] and was given two different interpretations: Lauret *et al.* assigned it to a red shift of the π-plasmon resonance [13], while Korovyanko *et al.* attributed it to transitions between the first and third conduction or valence subbands [14]. These transitions, strictly forbidden within the tight-binding (TB) approximation, become allowed by considering excitonic effects. According to calculations [9], each exciton has a manifold of states, with different symmetry and dipole coupling, both below and above the respective band continuum. Since the energy of the PA ($\sim$2 eV) corresponds to the energy difference between the EX1 and EX3 transitions, we attribute it to a transition between the lowest EX1 level and a suitable level of the EX3 manifold with the appropriate symmetry, according to the selection rules.

The inset in Fig. 2(b) shows PA recovery on a longer time scale: The signal is modulated by an oscillatory pattern due to coherent vibrational motion initiated by the pump pulse. The Fourier transform of the oscillatory component indicates a frequency of 259 cm^{-1}, corresponding to the radial breathing mode (RBM) of semiconducting SWNTs, as it is possible to see in the Raman

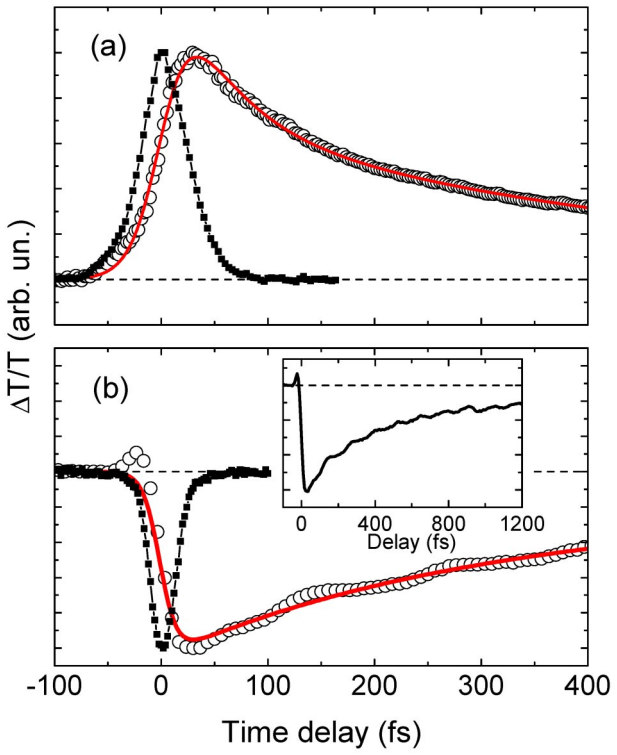

FIG. 2 (color online). (a) $\Delta T/T$ dynamics of SWNTs excited at 0.92 eV and probed at 0.95 eV (circles) together with fit (solid line) and pump pulse autocorrelation (squares + line); (b) same as (a) but at 2 eV probe wavelength and with pump-probe cross correlation. Inset shows the measurement on a longer time scale.

spectrum [22]. Time domain detection of the RBM suggests a strong coupling of the localized exciton state with the lattice vibrations. The RBM frequency and the fact that the primary excitation was at 0.92 eV allow one to identify the nanotubes excited in the experiments. On the basis of TB calculations parametrized for the assignment of the Raman spectra [24], one finds that the (10, 3), (11, 1), (9, 4), and (7, 6) SWNTs are excited, with the first excitation at 0.87, 0.88, 0.92, and 0.92 eV and RBM frequencies [25] at 253, 258, 257, and 263 cm^{-1}, in the ground state, respectively.

Figure 3 shows $\Delta T/T$ dynamics following excitation with a sub-10 fs visible pulse, resonant with the EX2 transition of semiconducting SWNTs and with the first excited state of metallic SWNTs. In a degenerate measurement, at 2.15 eV probe energy one observes an instantaneously rising positive signal, due to PB of the EX2 transition [Fig. 3(b)]; it decays within $\approx$ 150 fs into a PA similar to the one observed with the pump at 0.92 eV. The PB decay and subsequent PA formation are assigned to EX2 $\rightarrow$ EX1 exciton relaxation, here temporally resolved for the first time. Fitting by a three-level model, after deconvolution of the pump-probe cross correlation, gives a time constant $\tau = 40 \pm 3$ fs for this process. Note that, also in this case, the PA is modulated by an oscillatory

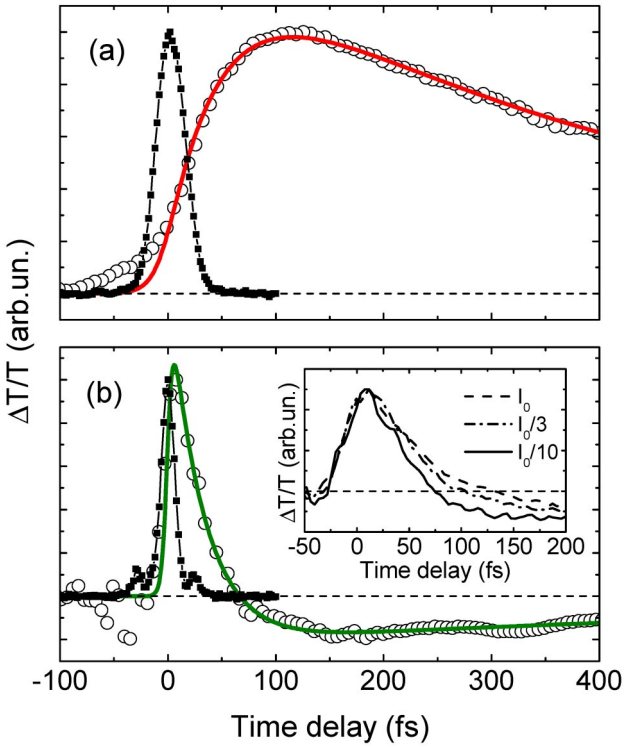

FIG. 3 (color online). (a) $\Delta T/T$ dynamics of SWNTs excited in the visible and probed at 0.92 eV (circles) together with fit (solid line) and pump-probe cross correlation (squares + line); (b) same as (a) but at 2.15 eV probe energy and with pump pulse autocorrelation. Inset of Fig. 3(b) shows intensity dependence of the dynamics at 2.15 eV.

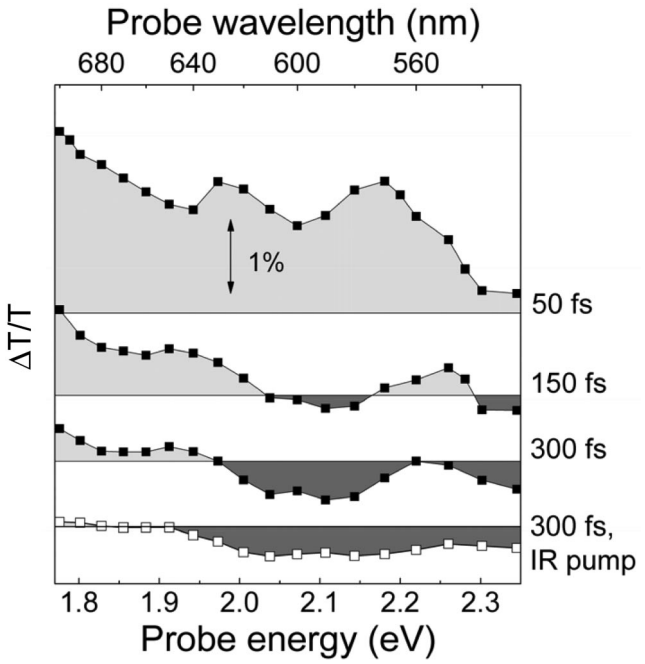

FIG. 4. $\Delta T/T$ spectra of SWNTs excited by a sub-10 fs visible pulse at different pump-probe delays. The lower panel also shows a $\Delta T/T$ spectrum with IR excitation (0.92 eV).

signal due to the impulsively excited RBM at 246 cm^{-1}. Our interpretation is confirmed by measurements at 0.95 eV probe energy [Fig. 3(a)]. In this case the PB of the EX1 transition shows a delayed rise, with a time constant of 40 fs, due to population buildup. Dynamics of exciton relaxation can be better visualized by $\Delta T/T$ spectra at different time delays, following visible excitation (see Fig. 4). At early times (50 fs delay) one observes the PB spectrum of the EX2 transition, which then rapidly decays to form the PA of EX1. In the same figure the $\Delta T/T$ spectrum measured with IR excitation (0.92 eV) is reported, showing a PA band with shape similar to the one obtained with visible excitation; this supports the assignment of the visible PA band to a transition from EX1. The sub-10 fs visible pulse can excite many more nanotubes than that in the IR. However, the selection operated by the oxidation restricts the number of accessible ones. One finds that the semiconducting nanotubes that can be excited are (10, 3), (9, 5), (9, 4), and (7, 6) with RBM frequencies 253, 242, 257, and 263 cm^{-1} in the ground state and the second excitation at 1.95, 1.85, 2.03, and 1.92 eV, respectively [25]. This justifies the observation of oscillations with frequencies around 250 cm^{-1}.

Our broad visible excitation spectrum overlaps also partially with the absorption of the metallic SWNTs, leading to the question of whether they contribute to the ultrafast relaxation observed in the visible. Lack of coherent phonons around 200 cm^{-1}, which is the RBM frequency for metallic SWNTs [22], suggests that their contribution is negligible. To study this issue, we tuned our excitation to the red, using slightly longer pulses, in order to be more selective. Figure 5(a) shows the result of a degenerate measurement using 15 fs excitation pulses at 1.35 eV, resonant exclusively with the EX2 transition of the semiconducting SWNTs [25]; again we see a PB signal rising instantaneously and decaying with a time constant of 35 fs, confirming that this fast decay is due to relaxation out of EX2 in the semiconducting SWNTs. Finally, Fig. 5(b) shows a measurement performed using 15 fs blue pump pulses (2.75 eV), resonant with the third transition of the semiconducting SWNTs (EX3), and probing in the visible at 2.1 eV. This wavelength corresponds to the PB of the EX2 transition but also to the PA from EX1. Here we observe the buildup of a PA signal, indicating the population of the EX1 state; this corresponds to energy relaxation from EX3 into the lowest available state. In this case the time constant for the EX3 $\rightarrow$ EX1 relaxation process is 65 fs. The larger excess energy to be dissipated accounts for the longer time required.

The ultrafast relaxation of EX2 cannot derive from the bimolecular recombination because of the weak intensity dependence of the dynamics [see inset of Fig. 3(b)], which becomes slightly slower for higher excitation density. It

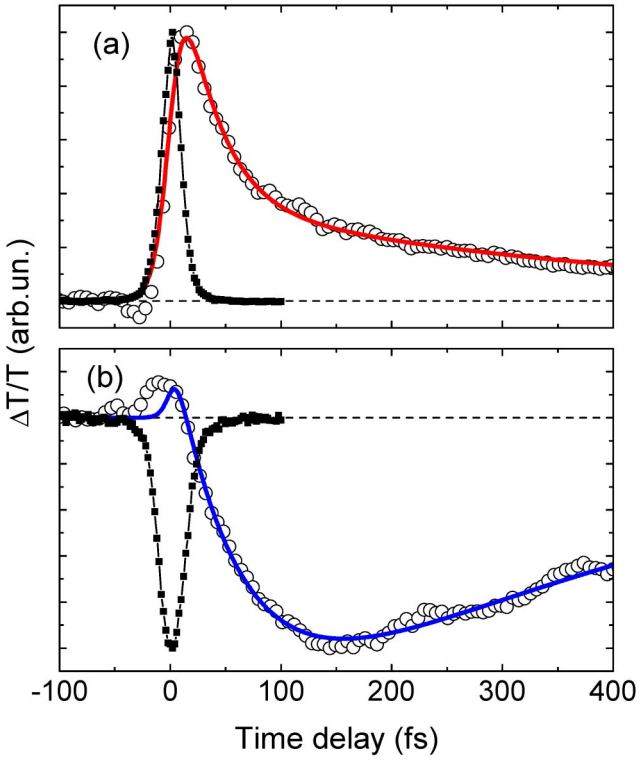

FIG. 5 (color online). (a) $\Delta T/T$ dynamics of SWNTs excited at 1.35 eV and probed at 1.35 eV (circles) together with fit (solid line) and pump pulse autocorrelation (squares + line); (b) $\Delta T/T$ dynamics of SWNTs excited at 2.75 eV and probed at 2.1 eV (circles) together with fit (solid line) and pump-probe cross correlation (squares + line).

can be understood within the semiconductor picture as a Fano resonance of the initial EX2 level with the continuum of the lower lying EX1 state. Common in inorganic low dimensional semiconductors [26], such resonances have recently been predicted for SWNTs too [27]. In particular, from the width of the calculated Fano line shape, a lifetime of 50 fs has been estimated for a semiconducting SWNT [28], in excellent agreement with our measurement. Because of the large phonon energy available, thermalization of hot EX1 can be very effective. The slower kinetics at higher density can be due to quenching of the phonon emission rate by the growing population (phonon bottleneck). These results are also consistent with a molecular picture in which EX2 undergoes an internal conversion to EX1 dressed by a phonon cloud. This suggests a comparison with other 1D systems, such as conjugated polymers, in which the internal conversion of higher lying excitons has a time constant of 45 fs [29], close to the one found here.

In conclusion, we have studied with unprecedented temporal resolution the dynamics of photoexcited excitons in SWNTs. Early exciton relaxation from higher levels is concluded in 150 fs, with a time constant of the order of $\tau = 40$ fs. This dynamics is consistent with the conjecture that primary excitations in SWNTs are excitons, i.e., geminate electron-hole pairs, confined by the 1D topology. We showed that correlated PB and PA bands exist, as predicted by theoretical models that include electron-electron interaction. Because of the concentration of oscillator strength induced by confinement in the 1D space, SWNTs are predicted to have very large nonlinear optical absorption [30]; this, in combination with the very fast recovery times we measured, makes them ideal candidates for an ultrafast all-optical switching application at frequencies well in excess of 1 THz.

[1] M. S. Dresselhaus, G. Dresselhaus, and Ph. Avouris, *Carbon Nanotubes: Synthesis, Structures and Applications* (Springer-Verlag, Berlin, 2001).
[2] M. M. J. Treacy, T. W. Ebbesen, and J. M. Gibson, Nature (London) **381**, 678 (1996).
[3] S. J. Tans, A. R. M. Verschueren, and C. Dekker, Nature (London) **393**, 49 (1998).
[4] A. Bachtold *et al.*, Science **294**, 1317 (2001).
[5] O. E. Alon, V. Averbukh, and N. Moiseyev, Phys. Rev. Lett. **85**, 5218 (2000).
[6] F. Rossi and E. Molinari, Phys. Rev. Lett. **76**, 3642 (1996); S. Abe, J. Phys. Soc. Jpn. **58**, 62 (1989).
[7] M. J. O'Connel *et al.*, Science **297**, 593 (2002); S. M. Bachilo *et al.*, Science **298**, 2361 (2002).
[8] C. L. Kane and E. J. Mele, Phys. Rev. Lett. **90**, 207401 (2003).
[9] H. Zhao and S. Mazumdar, Phys. Rev. Lett. **93**, 157402 (2004).
[10] T. Hertel and G. Moos, Phys. Rev. Lett. **84**, 5002 (2000).
[11] Y.-C. Chen *et al.*, Appl. Phys. Lett. **81**, 975 (2002).
[12] H. Han *et al.*, Appl. Phys. Lett. **82**, 1458 (2003).
[13] J.-S. Lauret *et al.*, Phys. Rev. Lett. **90**, 057404 (2003).
[14] O. J. Korovyanko *et al.*, Phys. Rev. Lett. **92**, 017403 (2004).
[15] G. N. Ostojic *et al.*, Phys. Rev. Lett. **92**, 117402 (2004).
[16] L. Huang, H. N. Pedrosa, and T. D. Krauss, Phys. Rev. Lett. **93**, 017403 (2004).
[17] Y.-Z. Ma *et al.*, J. Chem. Phys. **120**, 3368 (2004).
[18] F. Wang *et al.*, Phys. Rev. Lett. **92**, 177401 (2004).
[19] G. Cerullo and S. De Silvestri, Rev. Sci. Instrum. **74**, 1 (2003).
[20] M. Zavelani-Rossi *et al.*, Opt. Lett. **26**, 1155 (2001).
[21] F. Della Negra, M. Meneghetti, and E. Menna, Fuller. Nanotub. Carbon Nanostructures **11**, 25 (2003).
[22] E. Menna, F. Della Negra, M. Dalla Fontana, and M. Meneghetti, Phys. Rev. B **68**, 193412 (2003).
[23] A. G. Souza Filho *et al.*, Nanotechnology **14**, 1130 (2003); J. L. Bahr *et al.*, J. Am. Chem. Soc. **123**, 6536 (2001).
[24] A. Jorio *et al.*, Phys. Rev. Lett. **86**, 1118 (2001).
[25] C. Fantini *et al.*, Phys. Rev. Lett. **93**, 147406 (2004).
[26] C. P. Holfeld *et al.*, Phys. Rev. Lett. **81**, 874 (1998).
[27] C. D. Spataru *et al.*, Phys. Rev. Lett. **92**, 077402 (2004).
[28] C. D. Spataru *et al.*, Appl. Phys. A **78**, 1129 (2004).
[29] C. Gadermaier *et al.*, Chem. Phys. Lett. **384**, 251 (2004).
[30] Vl. A. Margulis, J. Phys. Condens. Matter **11**, 3065 (1999).